

## Gettering of Pd to implantation-induced nanocavities in Si

D. A. Brett, G. de M. Azevedo, D. J. Llewellyn, and M. C. Ridgway

Citation: *Applied Physics Letters* **83**, 946 (2003); doi: 10.1063/1.1597424

View online: <http://dx.doi.org/10.1063/1.1597424>

View Table of Contents: <http://scitation.aip.org/content/aip/journal/apl/83/5?ver=pdfcov>

Published by the [AIP Publishing](#)

---

### Articles you may be interested in

[Effects of surface oxide layer on nanocavity formation and silver gettering in hydrogen ion implanted silicon](#)  
*J. Appl. Phys.* **114**, 023502 (2013); 10.1063/1.4812736

[Trapping of Pd, Au, and Cu by implantation-induced nanocavities and dislocations in Si](#)  
*Appl. Phys. Lett.* **88**, 222107 (2006); 10.1063/1.2208382

[Gettering of copper in silicon at half of the projected ion range induced by helium implantation](#)  
*J. Appl. Phys.* **91**, 69 (2002); 10.1063/1.1418005

[Copper gettering at half the projected ion range induced by low-energy channeling He implantation into silicon](#)  
*Appl. Phys. Lett.* **77**, 972 (2000); 10.1063/1.1289062

[The role of oxygen on the stability of gettering of metals to cavities in silicon](#)  
*Appl. Phys. Lett.* **75**, 2424 (1999); 10.1063/1.125035

---

The advertisement features a dark blue background with a light blue gradient on the left. On the left side, the text 'Model PS-100' is in a large, bold, white font, with 'Tabletop Cryogenic Probe Station' below it in a smaller white font. In the center, there is a detailed image of the Model PS-100 cryogenic probe station, showing various mechanical components and a probe tip. On the right side, the 'Lake Shore CRYOTRONICS' logo is displayed, with 'Lake Shore' in a large, white, serif font and 'CRYOTRONICS' in a smaller, white, sans-serif font below it. Below the logo, the tagline 'An affordable solution for a wide range of research' is written in a white, italicized serif font.

## Gettering of Pd to implantation-induced nanocavities in Si

D. A. Brett,<sup>a)</sup> G. de M. Azevedo, D. J. Llewellyn, and M. C. Ridgway

*Department of Electronic Materials Engineering, Research School of Physical Sciences and Engineering, Australian National University, Canberra ACT 0200 Australia*

(Received 2 May 2003; accepted 12 June 2003)

The gettering of Pd to nanocavities in Si for implantation doses ranging from  $5 \times 10^{13}$  to  $1 \times 10^{15} \text{ cm}^{-2}$  and annealing temperatures ranging from 750 to 1050 °C was investigated using Rutherford backscattering and cross-sectional transmission electron microscopy. For a given annealing temperature, the gettering efficiency increased as the dose decreased. For a given dose, maximum gettering efficiency was achieved at the intermediate temperatures studied. Competition between silicide formation and nanocavity gettering limited gettering efficiency. © 2003 American Institute of Physics. [DOI: 10.1063/1.1597424]

Transition metal contamination can inject undesired deep levels, reduce minority carrier lifetime, and impede the proper functioning of Si devices.<sup>1</sup> However, nanocavities formed in Si by H or He implantation and subsequent annealing are effective in gettering a number of transition metals, including Ni,<sup>2</sup> Cu,<sup>3</sup> Ag,<sup>4</sup> Pt,<sup>4</sup> and Au.<sup>5</sup> It is the dangling bonds on the inner surface of such nanocavities that form attractive trapping or gettering sites for these metallic impurities.<sup>6</sup> Nanocavities can trap metal contaminants outside the device active region, yet may be formed on the device side of the wafer, making them potentially useful for proximity gettering. In this letter, we investigate the gettering of Pd to implantation-induced nanocavities in Si. This report on the interaction between Pd and nanocavities is timely, given that this transition metal has potential applications in device manufacture, for instance as a component of an interconnect alloy.<sup>7</sup> By investigating a range of doses and annealing temperatures, we explore the relationship between Pd gettering efficiency and the processing parameters.

A single nanocavity band was formed in (100) Czochralski Si wafers by room temperature implantation of 30 keV H<sup>-</sup> ions (with a projected range of  $\sim 380 \text{ nm}$ )<sup>8</sup> to a dose of  $3 \times 10^{16} \text{ cm}^{-2}$ . This was followed by annealing for 1 h at 850 °C under flowing Ar to induce nanocavity formation. The nanocavities thus produced had an average diameter of  $\sim 10 \text{ nm}$  and a surface area corresponding to an areal dose of  $1 \times 10^{14} \text{ cm}^{-2}$ .<sup>3</sup> Pd was then introduced into the samples by room temperature implantation of 235 keV Pd<sup>+</sup> ions (with a projected range of  $\sim 110 \text{ nm}$ ) to doses ranging from  $5 \times 10^{13}$  to  $1 \times 10^{15} \text{ cm}^{-2}$ . This implant was followed by an anneal for 1 h under flowing Ar at temperatures ranging from 750 to 1050 °C, to enable Pd diffusion and induce gettering. The samples were then analyzed by random-orientation Rutherford backscattering (RBS) with 1.6 MeV He<sup>+</sup> ions and a scattering angle of 168°. Cross-sectional transmission electron microscopy (XTEM) analysis was performed on selected samples using a Phillips CM-300 microscope operating at 300 kV.

Figure 1 shows RBS spectra of a  $5 \times 10^{14} \text{ Pd cm}^{-2}$  im-

plant before and after annealing at 950 °C. Before annealing, the implanted Pd is centered at a depth of  $\sim 120 \text{ nm}$ , consistent with the range predicted by SRIM 2000. Subsequent to annealing, the Pd has clearly redistributed from the implant region to a depth of  $\sim 390 \text{ nm}$ . The fraction gettered under these conditions is  $(51 \pm 4)\%$ . XTEM confirmed the presence of a nanocavity band centered at a depth of  $\sim 385 \text{ nm}$ , corresponding with the peak of the H implant distribution predicted by SRIM 2000, and the depth at which RBS analysis indicated the presence of gettered Pd. This was consistent with previous work that showed nanocavities form at the peak of the implant distribution.<sup>6</sup> The micrograph of Fig. 2 is taken from a  $1 \times 10^{15} \text{ Pd cm}^{-2}$  implant annealed at 950 °C for 1 h and shows at least two nanocavities with evidence of crystalline precipitates. The moiré patterns were consistent with PdSi, the most Si-rich silicide phase observed following thermal annealing of Pd layers on Si at atmospheric pressure.<sup>9</sup> Nonetheless, for the experimental uncertainty associated with the moiré fringe analysis, Pd<sub>2</sub>Si could not be excluded as a possibility.

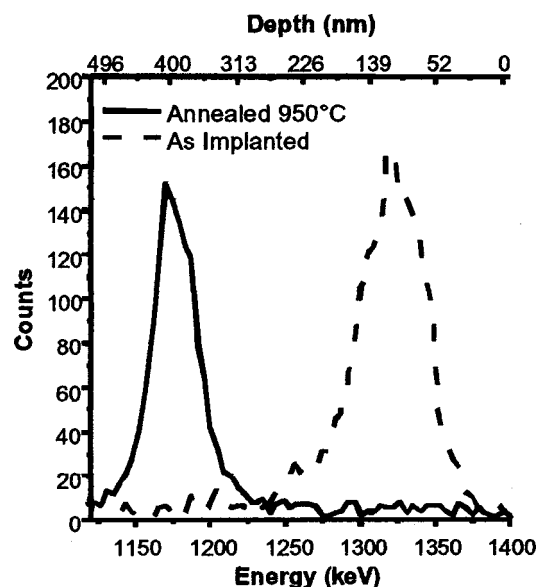


FIG. 1. RBS spectra of backscattered ion counts as functions of backscattered ion energy and depth below the surface of a 235 keV,  $5 \times 10^{14} \text{ Pd cm}^{-2}$  implanted sample both before and after annealing at 950 °C for 1 h.

<sup>a)</sup>Author to whom correspondence should be addressed; electronic mail: dab109@rphysse.anu.edu.au

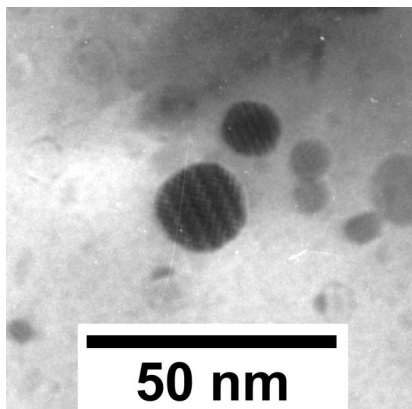


FIG. 2. Micrograph of a 235 keV  $1 \times 10^{15}$  Pd  $\text{cm}^{-2}$  implanted sample following annealing at 950 °C for 1 h. Note the nanocavities containing moiré fringes at the center of the image.

In Fig. 3 the gettering efficiencies as functions of Pd dose and annealing temperature are shown. For all doses, gettering efficiency is a maximum at an intermediate annealing temperature: the gettering efficiency is lower for annealing at 750 and 1050 °C and higher for annealing at 850 and 950 °C. The optimum temperature for maximum gettering efficiency increases as the Pd dose increases. At 750 °C, Pd was detected at a depth of  $\sim 90$  nm for all doses, up to  $\sim 98\%$  of the total in the case of the  $1 \times 10^{15}$   $\text{cm}^{-2}$  implant, despite a diffusion length of  $\sim 2$   $\mu\text{m}$  for Pd at this temperature and annealing time.<sup>10</sup> This Pd was closer to the surface than originally implanted, suggesting Pd segregated during the solid-phase epitaxial regrowth (SPEG) of the Si layer amorphized by the Pd implant. For the lowest dose, amorphization was incomplete and a lesser fraction of Pd was detected at  $\sim 90$  nm. To better understand the accumulation of Pd at such depths, selected samples were implanted at 300 °C. The gettering efficiency was improved by implanting Pd at 300 °C. This suggests segregated Pd may form a silicide during or subsequent to SPEG, and this silicide phase must be dissolved to enable gettering at the nanocavities. This difficulty in relocating Pd from the implant region to the nanocavities

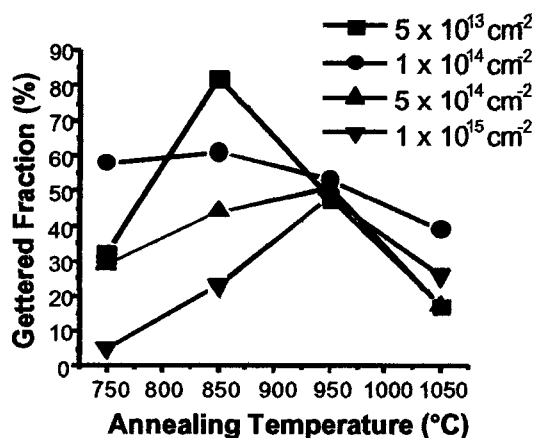


FIG. 3. RBS data showing the gettering efficiency as a function of Pd dose and annealing temperature. Values are accurate to within  $\pm 26$  for  $5 \times 10^{13}$  Pd  $\text{cm}^{-2}$ ,  $\pm 14$  for  $1 \times 10^{14}$  Pd  $\text{cm}^{-2}$ , and  $\pm 4$  for both  $5 \times 10^{14}$  Pd  $\text{cm}^{-2}$  and  $1 \times 10^{15}$  Pd  $\text{cm}^{-2}$ .

was not unexpected—similar observations have been reported for Ni<sup>2</sup> and Pt.<sup>4</sup> Given Pd, Ni, and Pt readily form silicides, silicide formation competes with nanocavity gettering. This is in contrast to other metals, such as Cu or Au, which do not readily form silicides, and exhibit much higher gettering efficiencies.<sup>10,11</sup> At the annealing temperature of 850 °C, only the RBS spectrum of the  $1 \times 10^{15}$   $\text{cm}^{-2}$  implant showed detectable amounts of Pd near the surface ( $\sim 45$  nm), and none could be detected at 950 °C. We attribute such results to increased diffusivity, solubility and silicide dissolution. At 1050 °C, the gettering efficiency is lower for all doses and Pd is broadly distributed between the cavity band and the surface. This suggests Pd may have redistributed away from the nanocavity band at this temperature. Possible causes for such behavior at this temperature include gettering of O from within Czochralski Si with subsequent ejection of previously trapped metal,<sup>12</sup> nanocavity instability,<sup>13</sup> and metal detrapping from nanocavity walls due to thermal excitation.<sup>14</sup> In general, the amount of Pd *not* located in the nanocavities or in the implant region was *below* the calculated solubility of Pd at the annealing temperatures,<sup>9,15</sup> thus indicating that nanocavities are an efficient sink for Pd.

In conclusion, we have demonstrated that nanocavities in Si can effectively getter Pd. The efficiency of this process was greatest at intermediate annealing temperatures and increased as the Pd dose decreased. The gettering efficiency of the nanocavities is adversely affected by Pd silicide formation. These results will aid in further studies of the interaction between transition metals and nanocavities in Si.

The authors thank the Australian Research Council for their financial support. G.deM.A. acknowledges the Brazilian agency CNPq (Conselho Nacional de Desenvolvimento Científico e Tecnológico) for a postdoctoral fellowship.

<sup>1</sup> K. Graff, Mater. Sci. Eng., B **4**, 63 (1989).

<sup>2</sup> B. Mohadjeri, J. S. Williams, and J. Wong-Leung, Appl. Phys. Lett. **66**, 1889 (1995).

<sup>3</sup> J. Wong-Leung, C. E. Ascheron, M. Petracic, R. G. Elliman, and J. S. Williams, Appl. Phys. Lett. **66**, 1231 (1995).

<sup>4</sup> A. Kinomura, J. S. Williams, J. Wong-Leung, and M. Petracic, Nucl. Instrum. Methods Phys. Res. B **127/128**, 297 (1997).

<sup>5</sup> J. Wong-Leung, J. S. Williams, and E. Nygren, Nucl. Instrum. Methods Phys. Res. B **106**, 424 (1995).

<sup>6</sup> J. S. Williams, M. C. Ridgway, M. C. Conway, J. Wong-Leung, X. Zhu, M. Petracic, F. Fortuna, M.-O. Ruault, H. Bernas, A. Kinomura, Y. Nakano, and Y. Hayashi, Nucl. Instrum. Methods Phys. Res. B **178**, 33 (2001).

<sup>7</sup> A. G. Dirks, R. A. Augur, and A. E. M. de Veirman, Thin Solid Films **246**, 164 (1994).

<sup>8</sup> J. F. Ziegler, J. P. Biersack, and U. Littmark, *The Stopping and Range of Ions in Solids* (Pergamon, New York, 1985).

<sup>9</sup> W. Schröter and M. Seibt, in *Properties of Crystalline Silicon*, edited by R. Hull (INSPEC, London, 1998), No. 20, pp. 543–560.

<sup>10</sup> K. Graff, *Metal Impurities in Silicon-Device Fabrication*, 2nd ed. (Springer, Berlin, 2000).

<sup>11</sup> J. Wong-Leung, J. S. Williams, A. Kinomura, Y. Nakano, Y. Hayashi, and D. J. Eaglesham, Phys. Rev. B **59**, 7990 (1999).

<sup>12</sup> J. S. Williams, M. Conway, J. Wong-Leung, P. N. K. Deenapanray, M. Petracic, R. A. Brown, D. J. Eaglesham, and D. C. Jacobson, Appl. Phys. Lett. **75**, 2424 (1999).

<sup>13</sup> X. Zhu, J. S. Williams, D. J. Llewellyn, and J. C. McCallum, Appl. Phys. Lett. **74**, 2313 (1999).

<sup>14</sup> V. Raineri, P. G. Fallica, G. Percolla, A. Battaglia, M. Barbagallo, and S. U. Campisano, J. Appl. Phys. **78**, 3727 (1995).

<sup>15</sup> K. Graff, H.-A. Hefner, and H. Pieper, Mater. Res. Soc. Symp. Proc. **36**, 19 (1985).